



Published in final edited form as:

*Mol Microbiol.* 2012 February ; 83(3): 654–664. doi:10.1111/j.1365-2958.2011.07958.x.

## Polar Assembly and Scaffolding Proteins of the Virulence-Associated ESX-1 Secretory Apparatus in Mycobacteria

Samantha E. Wirth<sup>1</sup>, Janet A. Krywy<sup>2</sup>, Bree Aldridge<sup>3</sup>, Sarah Fortune<sup>3</sup>, Marta Fernandez-Suarez<sup>3</sup>, Todd A. Gray<sup>1,2</sup>, and Keith M. Derbyshire<sup>1,2,\*</sup>

<sup>1</sup>Division of Genetics, Wadsworth Center, Center for Medical Science, New York State, Department of Health, Albany, NY 12201, USA

<sup>2</sup>Department of Biomedical Sciences, School of Public Health, State University of New York at Albany, Albany, NY 12201-2002, USA

<sup>3</sup>Department of Immunology and Infectious Disease, Harvard School of Public Health, Boston, MA, USA

### Summary

The ESX-1 secretion system is required for pathogenicity of *Mycobacterium tuberculosis* (*Mtb*). Despite considerable research, little is known about the structural components of ESX-1, or how these proteins are assembled into the active secretion apparatus. Here, we exploit the functionally related ESX-1 apparatus of *Mycobacterium smegmatis* (*Ms*) to show that fluorescently tagged proteins required for ESX-1 activity consistently localize to the cell pole, identified by time-lapse fluoro-microscopy as the non-septal (old) pole. Deletions in *Msesx1* prevented polar localization of tagged proteins, indicating the need for specific protein-protein interactions in polar trafficking. Remarkably, expression of the *Mtb* *esx1* locus in *Msesx1* mutants restored polar localization of tagged proteins, indicating establishment of the *Mtb* ESX-1 apparatus in *M. smegmatis*. This observation illustrates the cross-species conservation of protein interactions governing assembly of ESX-1, as well as polar localization. Importantly, we describe novel non-*esx1* encoded proteins that affect ESX-1 activity, that co-localize with ESX-1, and that are required for ESX-1 recruitment and assembly. This analysis provides new insights into the molecular assembly of this important determinant of *Mtb* virulence.

### Keywords

ESX-1; Mycobacteria; Protein localization; Secretion

### Introduction

Bacteria utilize secretion systems to move substrates across the barriers presented by the cell membrane and/or cell wall (Christie *et al.*, 2005, Papanikou *et al.*, 2007, Hayes *et al.*, 2010). The secretion of protein substrates is required for bacteria to decorate their surfaces with receptors and ligands, and to secrete effectors into their environment. The target of these effectors can either be other bacteria or eukaryotic cells, depending on the bacterium's lifestyle. For bacterial pathogens, secretion systems have become essential for their ability to survive, replicate and disseminate in their hosts. For example, the *Legionella pneumophila*

\*Correspondence should be addressed to: Keith M. Derbyshire, Telephone: 518-473-6079, Fax: 518-474-3181, keith.derbyshire@wadsworth.org.

Icm/Dot Type IV secretion system secretes over 250 substrates, some of which contribute to establishment of a successful infection and subsequent pathogenesis (Zhu *et al.*, 2011).

Seven secretion systems have been described thus far, each distinguished by hallmarks in their structures or functions (Tseng *et al.*, 2009). The Type VII Secretion Systems (T7SS) were originally described in the pathogen *Mycobacterium tuberculosis* (*Mtb*), which encodes five related, but functionally distinct, T7SS (Gey Van Pittius *et al.*, 2001, Pallen, 2002). Each apparatus is encoded by a large multigene locus named *esx1-5*, which expresses related sets of proteins, although they do not cross complement (Abdallah *et al.*, 2007, DiGiuseppe Champion and Cox, 2007). The archetypal T7SS is the ESX-1 secretory apparatus of *Mtb* (Bitter *et al.*, 2009). Interest in *Mtb* ESX-1 was further intensified by the finding that a deletion of seven *esx1* genes is the primary attenuating mutation in the avirulent *M. bovis* vaccine strain, BCG (Fig. 1B; (Behr *et al.*, 1999, Mahairas *et al.*, 1996). This conclusion has been widely corroborated, with a role for ESX-1 being linked to bacterial survival in host macrophages (Behr *et al.*, 1999, Hsu *et al.*, 2003, Lewis *et al.*, 2003, Mahairas *et al.*, 1996, Pym *et al.*, 2002).

Exactly how *Mtb* ESX-1 promotes pathogenicity is unknown, although most hypotheses focus on the potential functions of the proteins encoded by genes within the *esx1* locus, which are required for the survival and dissemination of *Mtb* in the host (Simeone *et al.*, 2009). The primary substrate secreted by ESX-1 is a heterodimeric product of the tandem *esxB* and *esxA* genes (Berthet *et al.*, 1995, Renshaw *et al.*, 2002). Efforts to comprehensively identify all ESX-1 substrates are complicated by the apparent absence of a distinct secretion signal, and the mutually dependent secretion of the majority of known secreted proteins: EsxAB secretion is dependent on the co-secretion of proteins encoded from both *esx1* (eg., EspE) and non-*esx1* genes (eg., EspA; (Fortune *et al.*, 2005, MacGurn *et al.*, 2005).

The structure of the secretory apparatus itself is also poorly defined. Current models of ESX-1 structure have largely been inferred by determining which genes are conserved within homologous *esx* loci (called Ecc for **E**sx **c**onserved **c**omponent), followed by analyses of the encoded proteins to identify features such as transmembrane domains and protein-protein interactions (Fig. 1A; Bitter *et al.*, 2009). Briefly, the trans-membrane protein EccD is thought to form the inner-membrane channel through which EsxAB are secreted. Substrate translocation through the channel is thought to be powered by the ATPase, EccC, which is often encoded by split genes *eccCa* and *eccCb*. It is difficult to directly interrogate how, and where, the apparatus components are assembled because of the thick, waxy layer of mycolic acids characteristic of mycobacteria outer-membranes. Thus far, the only in situ characterization of the assembled apparatus has been performed using an *M. marinum* *AkasB* strain defective in mycolic acid synthesis, which results in a more permeable cell wall, allowing an initial antibody-based approach to localizing exposed ESX-1 epitopes (Carlsson *et al.*, 2009). These studies suggested that the ESX-1 apparatus is localized to a bacterial pole. However, this immuno-fluorescence-based approach was limited to recognition of surface exposed epitopes and by having to use a mutant mycobacteria with a defective cell wall. Consequently, the majority of cytoplasmic components of the secretion apparatus cannot be visualized in their native context by this method.

In order to visualize the localization and assembly of the ESX-1 secretion apparatus, we have systematically expressed fluorescent-protein fusions of putative and candidate ESX-1 components in *M. smegmatis*: *esx1<sub>ms</sub>* is genetically and functionally conserved with that of *Mtb* (Fig. 1B; Coros *et al.*, 2008, Flint *et al.*, 2004, Converse and Cox, 2005). Analogous to its *Mtb* counterpart, ESX-1<sub>ms</sub> secretes a heterodimer of EsxAB<sub>ms</sub> (71% and 62% identical to the same proteins in *Mtb*). Here, we have used the *M. smegmatis* model system to track the intracellular localization (and co-localization) of ESX1 proteins in live cells and defined the

role that individual proteins, implicated in ESX-1 function, play in localization of ESX-1 components.

In *M. smegmatis*, ESX-1<sub>ms</sub> also regulates a novel type of conjugative DNA transfer, which we have previously exploited to identify genes required for ESX-1 activity (Coros et al., 2008, Flint et al., 2004). Here we demonstrate that a non-*esx1* operon (*Msmeg0044-0046*, which we rename *saeABC*), previously shown to be essential for ESX-1<sub>ms</sub> mediated secretion of EsxAB and for conjugal DNA transfer, is required for appropriate localization of core components of the apparatus. The discovery of a new locus necessary for ESX-1 recruitment to the pole will lead to a more comprehensive understanding of the structure and function of T7SS, and help to build an empirically determined model of the assembly and structure of ESX-1.

## Results

### ESX-1 associated proteins localize to the polar regions of *M. smegmatis* cells

In order to determine the cellular location of components associated with the ESX-1 secretion apparatus, *esx1*-associated genes were PCR amplified from the *M. smegmatis* mc<sup>2</sup>155 donor genome and fused, in frame, to a gene encoding a yellow fluorescent protein, YFP-Venus (Nagai et al., 2002). A penta-glycine chain was used as a linker joining the two proteins to reduce steric interference and allow native folding of the N-terminal ESX-1 protein. The genes were introduced into *M. smegmatis* on a plasmid and expressed from either the Hsp60 or the inducible Ptet promoter (Ehrt et al., 2005, Stover et al., 1991). In preliminary experiments, we established that expression of native YFP resulted in fluorescence distributed throughout the cell (Fig. 1C).

A previous study had shown that the *M. marinum* protein Mh3864 (EspE<sub>mm</sub>) is secreted and remains partially associated with the cell pole of the bacterium (Carlsson et al., 2009). We therefore investigated the cellular location of the *M. smegmatis* ortholog Msmeg0055 (EspE<sub>ms</sub>). Ectopic expression of EspE<sub>ms</sub> tagged at its C-terminus with YFP revealed that it, too, was localized to a pole of the mc<sup>2</sup>155 cell: cells had foci located at one or both cell poles (Fig. 1D). Our preliminary studies indicate EspE<sub>ms</sub> is not secreted, unlike its *M. marinum* counterpart, but its polar localization is consistent with the association of EspE<sub>ms</sub> with the ESX-1 apparatus.

We have established that ESX-1 activity is essential for DNA transfer and EsxAB secretion in the *M. smegmatis* recipient strain, MKD8 (Coros et al., 2008). We sought to determine whether polar localization also occurred in the recipient strain, or if it was a uniquely donor-encoded property. As with the donor strain, EspE<sub>ms</sub>-YFP was localized to the cell poles: 133/207 recipient cells examined contained polar foci and 86/133 had a single polar focus (Fig. S1A). We have since shown that all the fusion proteins described below localized to a pole in both donor and recipient and, therefore, we will focus on localization of ESX-1 in the donor strain (data for the recipient are shown in Fig. S2). Throughout these studies, we noted some variability in the percentage of cells containing fluorescent foci of a particular protein. For example, a higher percentage of recipient cells (41%) contained a single polar focus of EspE compared with the donor (24%). This implies there are growth, environmental and expression factors influencing protein production and assembly that we do not, as yet, understand. The precise location of the foci at the pole of the cell varied between a location at the tip apex to one near the onset of tip curvature (peripolar). We therefore use the term polar here to indicate at, or very close to, the cell pole.

As EspE<sub>ms</sub> was localized to the cell pole, we investigated whether other ESX-1-associated proteins would be similarly localized. EccCb<sub>ms</sub> (Msmeg0062) encodes an ftsk/spoIIIE

family ATPase that is central to ESX-1 function and, presumably, integral to its structure (Fig. 1A). EccCb<sub>ms</sub> was tagged with YFP-Venus and ectopically expressed in *M. smegmatis*. Localization of this ESX-1-associated protein was very similar to that of EspE: 47% (29/62) of fluorescent cells contained a single EccCb<sub>ms</sub> focus, localized to the polar region of the cell (Figs. 1E, S2E). Not all the ESX-1 proteins we tested were localized. For example, we examined N- and C-terminal fusions of YFP to secreted proteins EsxB<sub>ms</sub> and EsxA<sub>ms</sub>, respectively. In each case, and in both donor and recipient, the EsxA and EsxB fusion proteins were not localized (data not shown). This is not unexpected, as we would predict localization would be a property of structural components of the apparatus.

We next determined whether ESX-1 components from *Mtb* showed similar localization when heterologously expressed in *M. smegmatis*. EspE<sub>mt</sub> and EccCb<sub>mt</sub>, were similarly tagged and expressed in mc<sup>2</sup>155. In both cases, cells showed a polar focus of fluorescence (Figs. 1D, E, S3). This is consistent with the previous antibody studies, which indicated that EspE<sub>mm</sub> was localized to polar regions of the cell surface (Carlsson et al., 2009). These results suggest that the cellular proteins and signals necessary for determining the site of the ESX-1 apparatus are conserved among *M. marinum*, *M. smegmatis* and *M. tuberculosis*.

### Localization of EccCb<sub>ms</sub> is dependent on other ESX-1 proteins

We reasoned that protein localization of EccCb or other ESX-1 components reflects their incorporation into a macromolecular complex, and that in the absence of an intact apparatus these proteins would not localize appropriately. Therefore, proteins that showed distinct localization in wild-type *M. smegmatis* were used as reporters for assembly and localization of the apparatus in ESX-1 mutant backgrounds. As shown above, EccCb<sub>ms</sub>-YFP (as well as EccCb<sub>mt</sub>-YFP, Fig. 1E) primarily localized to a single cell pole when expressed in wild-type *M. smegmatis*. When EccCb<sub>ms</sub>-YFP was expressed in a mutant strain containing a large *esxI* deletion ( $\Delta 0056-0082$ ; Fig. 1B), this ESX-1 protein no longer localized to the cell pole (Fig. 2A). These data confirm that the localization of ESX-1-associated proteins is specific and not an artifact of protein aggregation or expression. EccCb<sub>ms</sub>-YFP must make specific contacts with *esxI*-encoded proteins that recruit it to the polar region. Current models of the ESX-1 apparatus posit that EccCb may be tethered through interactions with an integral membrane protein, EccCa (Fig. 1A; Abdallah et al., 2007). However, EccCb-YFP did not show polar localization in a background with a smaller deletion ( $\Delta eccCb-esxA$ ) encoding an intact EccCa<sub>ms</sub> (Fig. 2B). This observation indicates that the recruitment of EccCb<sub>ms</sub>-YFP to the cell pole requires other *esxI*-encoded proteins in addition to EccCa<sub>ms</sub>.

Functional conservation between the components of *M. smegmatis* and *Mtb*ESX-1 has been repeatedly observed. For example, inactivating transposon insertions in *M. smegmatis* *esxI* genes affect DNA transfer and can be ameliorated by complementation with a cosmid carrying *Mtb* genes (*Rv3861-Rv3885*), which encompasses the entire *Mtb**esx1* locus (*Rv3864-Rv3883*; Fig. 1B; Flint et al., 2004). Therefore, we assessed the ability of this *esxI*<sub>mt</sub> cosmid to complement the EccCb<sub>ms</sub> localization defect of the  $\Delta esxI$ <sub>ms</sub>. Expression of ESX-1<sub>mt</sub> restored polar localization of EccCb<sub>ms</sub> in the absence of ESX-1<sub>ms</sub> (Fig. 2C). This result further underscores the functional conservation of the ESX-1 apparatus between *M. smegmatis* and *Mtb*, and suggests that the *Mtb*ESX-1 apparatus is also recruited to, and assembled at, the cell pole, while incorporating EccCb<sub>ms</sub>-YFP.

In addition to the above experiments, we also assessed the ability of the EccCb-YFP-fusion to rescue conjugal DNA transfer to further demonstrate that the protein is expressed in a functional form. A transposon insertion in *eccCb*<sub>ms</sub> reduces transfer to undetectable levels (<1 transfer event per 10<sup>9</sup> donor cells). Expression of *eccCb*<sub>ms</sub>-YFP in the mutant background restored DNA transfer over 500-fold ( $5.5 \times 10^{-7}$  events per donor). Western analyses confirmed that the fusion protein was expressed at similar levels in both wild-type

and mutant backgrounds, and that there was minimal proteolytic cleavage of the full-length fusion protein (Fig S4). Together, these data suggest that the EccCb-YFP-fusion protein is functional and that fluorescent foci are sites of functional ESX-1 complexes containing intact EccCb-YFP.

### Non-*esx1* encoded proteins also localize to the cell poles of *M. smegmatis*

Transposon mutagenesis screens have identified genes that are not encoded from within the *esx1<sub>ms</sub>* genetic locus, yet are required for both ESX-1-dependent conjugal DNA transfer and EsxAB secretion (Coros et al., 2008, and this work). Non-*esx1*-encoded proteins may directly affect the structure of the ESX-1 apparatus itself, or through indirect means, as might be expected from a transcription factor or protein modification enzyme. In particular, we isolated multiple insertions in a three-gene operon, *Msmeg0044-0046* (which we will refer to as *saeA-C*), located 7-kb upstream from the start of the *esx1<sub>ms</sub>* locus (Fig. 3A). Ectopic expression of the last gene in this three-gene operon, SaeC, as a YFP-Venus fusion resulted in its discrete localization to a single polar region in the majority of fluorescing donor cells (Figs. 3B, C and S2H). This uni-polar localization is consistent with the localization of the *esx1*-encoded proteins described above, and suggests that proteins encoded in this non-*esx1* operon are also integral components of the ESX-1 secretory apparatus.

A precise deletion of *saeC* was created, and this mutation abolished EsxAB secretion (Fig 4), consistent with the known phenotype of *saeA* and *saeB* mutants (Coros et al., 2008). Deletion of *saeC* in the recipient strain abolished conjugal DNA transfer, but transfer was rescued over a 1000-fold by ectopic expression of either the wild-type or the fluorescently tagged SaeC to within 10-fold of wild-type levels (Table 1). This complementation is consistent with expression of a functional fluorescently tagged protein that is localized to a cell pole.

SaeA (Fig. 3D), but not SaeB (fusions of this protein were toxic to the cell), also localized to a cell pole, though its localization was conditional. When *M. smegmatis* was cultured in the presence of 0.05% Tween 80, SaeA-YFP did not localize to the poles; instead, cells appeared swollen with punctate fluorescence distributed throughout the cytoplasm (Fig. S1B). By contrast, growth in the absence of Tween 80 resulted in the localization of SaeA-YFP to the pole in both donor (Fig. 3D) and recipient cells (Figs. S2I-L). We examined the effect of Tween 80 on the other fusion proteins, but it had no effect on protein localization (data not shown). We speculate that the detergent properties of Tween 80, combined with overexpression of SaeA-YFP, alters the cell wall structure and perturbs ESX-1 assembly and localization.

### ESX-1 proteins co-localize at the cell pole

So far we have presented evidence that independent ESX-1-associated proteins localize to the polar region of *M. smegmatis*. In order to show that these proteins assemble at a specific and unique cellular location, we co-expressed proteins fused with differently fluorescing proteins. SaeC-YFP was co-expressed with either EspE<sub>ms</sub>-TdTomato or EccCb<sub>ms</sub>-TdTomato from a bi-cistronic episomal expression vector. In all cases (n=49), when dual fluorescence was observed within a cell it occurred at the same pole, as indicated by merging the images (Fig. 5). Importantly, SaeC co-localization with both EspE and EccCb shows that ESX-1 associated proteins, regardless of whether they are encoded within the *esx1* locus or elsewhere, traffic to the same location.



### ESX-1 primarily associates with the non-septal pole

In the majority of cells, the fluorescent ESX-1 components are observed at a single cell pole, suggesting that the poles are functionally distinct. To unambiguously evaluate polar identity, we compiled time-lapse fluoromicroscopy images of *M. smegmatis* ectopically expressing SaeC-YFP. We used live-cell imaging to follow the localization of SaeC over time in multiple, independent, clonal lineages. With image capture at 10 minute intervals, each cell division was observed, with a definitive assignment of each resulting “old” and “new” pole (Fig. 6 and Movie S1, Movie S2).

The fluorescence of the SaeC-YFP fusion is readily discernable in the time-lapse images and localizes to a single pole, in agreement with the conventional fluoromicroscopy images. Fig. 6 shows the division of two cells into four, and the appearance of three new foci. Initially, a single focus is observed at an old cell pole (black arrow) and this localized fluorescence remains associated with that pole following cell division at the septum (red arrow). Here, “old pole” is defined as the pole distal to the divisional septum (“new pole”). New fluorescent foci then appear in the other, previously non-fluorescing, daughter cells: in two of these daughter cells the foci are localized at the old pole (black arrows), while in the other daughter cell the protein is localized to the new pole (where division occurred). In 35/47 cells that had undergone cell division, in 8 independently monitored cell clusters, SaeC-YFP was localized to the old pole. Four foci appeared at the new pole, while the remaining foci (8) could not be properly assigned because there is increasing ambiguity due to cells clumping and moving as the cell number increased.

### SaeC is essential for polar localization of EccCb<sub>ms</sub>

As proteins encoded from the *saeA-C* operon are co-localized with ESX-1 proteins, we examined whether their localization was dependent on a complete ESX-1 apparatus. Surprisingly, SaeC-YFP was localized to the cell pole even in the absence of ESX-1 core components showing that its polar localization is independent of *esxI*-encoded proteins (Fig. 7A). Conversely, to determine whether *esxI*-encoded components are dependent on Sae proteins, EccCb<sub>ms</sub>-YFP localization was evaluated in a  $\Delta$ *saeA-C* mutant background. EccCb<sub>ms</sub>-YFP was not localized in this background, even though the *esxI* locus was intact (Fig. 7B). A similar phenotype was also observed in a mutant background with a precise deletion of *saeC* (Fig. 7C). Together, these data suggest that the SaeA-C proteins, and SaeC in particular, initiate an early step in the assembly of the *esxI*-encoded proteins at the pole. We also predict that the defect in DNA-transfer and EsxA/EsxB secretion in  $\Delta$ *sae* strains is because ESX-1 is either not assembled, or is mis-localized.

### Discussion

Despite the focused research on ESX-1 and related T7S systems, the composition of the secretion apparatus and the mechanism of secretion are still unknown. For example, in most cases, it is not known whether genes required for ESX-1 activity perform a structural role or modulate secretion through indirect regulatory contributions, such as chaperone activity. Protein localization will help to differentiate between these possibilities, and inform on how the secretion apparatus is assembled.

The fusion of monomeric fluorescent proteins, primarily YFP-Venus in this study, with proteins known to affect ESX-1 function, provides a non-invasive way to visualize where in the cell the secretion system is assembled. This study addresses fundamental questions concerning the ESX-1 secretion machine. Does a given Esx protein localize within the cell and, if so, does it co-localize with other ESX-1 proteins, suggesting it plays a structural role? If multiple ESX-1 structural (localized) proteins are used as reporters, can mutations in other

genes define the order-of-assembly of the apparatus? YFP fusions of two known *esxI*-encoded proteins, EspE<sub>ms</sub> and EccCb<sub>ms</sub>, revealed that these proteins localize to a single cell pole in the bacillus, corroborating a previous report in *M. marinum* with immunodetection of EspE<sub>mm</sub> and EccCa<sub>mm</sub> (Carlsson et al., 2009). Moreover, proteins encoded by a non-*esxI* operon, *saeA-C*, (*Msmeg0044-0046*), previously reported to affect ESX-1 function, are also polar localized. The use of two-color fluoromicroscopy showed that SaeC-YFP localized to the same pole as the *esxI*-encoded fusion proteins, consistent with its functional requirement for ESX-1 mediated secretion and DNA transfer activities. When EccCb<sub>ms</sub> was used as a reporter for ESX-1 assembly, we identified mutations that prevented its polar localization. This could be interpreted as the loss of a specific interaction needed to recruit EccCb<sub>ms</sub> to the secretion apparatus, or as dissolution of the apparatus itself. The use of other ESX-1 structural protein reporters will help to distinguish between these possibilities. Notably, deletion of *esxI* genes prevented assembly of EccCb<sub>ms</sub> at the cell pole indicating that other *esxI*-encoded proteins are necessary for localization. These proteins may act as chaperones or as scaffolds for the structural proteins.

Our demonstration that heterologous expression of the *MtbexxI* operon restored localization of EccCb<sub>ms</sub> in a  $\Delta$ *esxI*<sub>ms</sub> background implies that the *MtbexxI* locus recruited EccCb<sub>ms</sub> to the cell pole and further establishes the functional conservation of the ESX-1 apparatus between pathogenic and saprophytic species. This conservation is consistent with the hypothesis that the observed species-specific functional differences (e.g., virulence in *Mtb* or conjugation in *M. smegmatis*) are due to differences in secreted proteins, not differences in the secretory apparatus *per se*. By examining different combinations of YFP-reporter and *esxI* mutants, we are beginning to construct a hierarchical interaction map that outlines the potential protein interactions necessary to assemble and form the apparatus.

Localization of EccCb<sub>ms</sub> was also dependent on proteins encoded by *saeA-C*. This result, combined with the co-localization of SaeC with ESX-1 proteins, suggests that SaeA-C play a role as “keystones” in the *ESX-I*<sub>ms</sub> assembly process. Therefore, we propose that this operon be named the *sae* operon, reflecting the role of the genes (*saeABC*) in both the scaffolding and assembly of the ESX-1 apparatus. The proteins encoded by this operon have no close homologs in *Mtb*, suggesting that other proteins might perform the equivalent functional role in *Mtb*, and these are still to be discovered. Weak Sae homologs exist in more distantly related bacteria such as *Rhodococcus* and *Corynebacterium* species, but no function has been assigned to these hypothetical proteins and, as some of these species lack identifiable *esxI* genes, the homologs likely have evolved to perform different roles.

The approach used here has limitations in its application and interpretation. Some proteins appear to be refractory to this type of analysis, producing little or no fluorescent signal (*Msmeg0071*), inconsistent localization patterns, or sick cells (SaeB). While any protein can be tagged and expressed, an ~30 kDa tag may impede protein function or interaction with partner proteins. To address this, we have made both N- and C-terminal fusions, and used a penta-glycine linker joining the fluorescent protein with the target protein to minimize steric interference. Additionally, we have shown that fusion proteins are functionally active and that polar localization of the EccCb-YFP-fusion requires the *esxI* operon. Ectopic over-expression of fusion proteins might also contribute to toxicity issues, although we observed little improvement in the apparent health of the cells, or the intensity of the fluorescence using different promoters to drive protein expression (constitutive Hsp60 and inducible Ptet, data not shown). Indeed, the fact that foci were not visible in all cells for a given fusion protein (e.g. for EccCb-YFP, 37 out of 62 cells screened contained polar foci, while the remaining cells exhibited diffuse fluorescence; Fig. S2) indicates inherent heterogeneity in mycobacterial cultures and implies that not all cells have an assembled apparatus.

The non-invasive, real-time assay was exploited to determine the preferred site of ESX-1 assembly. Time-lapse imaging clearly showed that ESX-1 proteins prefer to locate at the “old” cell pole and not at the “new” septal pole. This interpretation differs from a previous report, which suggested that ESX-1 was positioned at the “new” pole (Carlsson et al., 2009). However, the discrepancy is not a disagreement of data, but results from the ambiguous terminology of “old” and “new” pole. Our time-lapse microscopy definitively discriminates between the pre-existing (old) pole, and that generated by septation (new pole). The confusion arises because mycobacteria, like other Actinobacteria, grow apically, i.e. new cell material is added at existing cell tips (old poles) and not at the developing septum (new poles) (Flardh, 2010). It is possible that the apparent peri-polar location of some foci is actually a consequence of the new growth transiently displacing the ESX-1 apparatus from the growing tip.

Unique cellular localization of macromolecular complexes is a common feature of cellular processes such as cell division and DNA replication, and secretion machines are no exception (Burton and Dubnau, 2010). The type IV secretion systems encoded by *Agrobacterium tumefaciens* and *Helicobacter pylori* are known to assemble at the cell poles (Burton and Dubnau, 2010, Judd et al., 2005, Kutter et al., 2008). Competence proteins responsible for uptake of DNA in *Bacillus subtilis* are also localized to the cell pole, as is the conjugation machinery necessary for transfer of ICEBs1 in *B. subtilis* and pSVH1 in *Streptomyces* (Hahn et al., 2005, Kaufenstein et al., 2011, Reuther et al., 2006). Although the cell pole seems to be a preferred site of DNA translocation in many species and even for attachment of mycobacteriophage (Edgar et al., 2008), so far there is no evidence suggesting that DNA transfer occurs at the growing pole during mycobacterial conjugation. ESX-1 is required for recipient activity, but we do not know whether the ESX-1 apparatus directly mediates DNA uptake. Moreover, *esxI* donor mutants are hyper-conjugative indicating ESX-1 suppresses, and does not transport DNA out of the donor cell.

Currently, there is an interesting debate on how a polar site is recognized by a protein. Most recently, localization of several proteins has been suggested to be mediated by their ability to recognize membrane curvature i.e., geometry is the determining factor (Ramamurthi, 2010, Lenarcic et al., 2009, Ramamurthi et al., 2009). However, others have shown that polar-localized proteins needed for DNA uptake in *B. subtilis* localize to discrete foci even in spheroplasts that have lost their rod shape (Kaufenstein et al., 2011). In the case of mycobacteria, the answer appears to be more complex. The majority of cells contained only one focus implying asymmetry of the poles and indicating localization was not simply determined by membrane curvature. This observation was reinforced by the time-lapse microscopy experiments, which showed that the old pole was the preferred site of assembly. As cell wall synthesis is occurring at this pole, this process, or a component of it, might be the signal that dictates ESX-1 localization. Furthermore, SaeC-YFP localization was independent of *esxI*-encoded proteins (SaeC-YFP was localized in an *esxI* deletion mutant), yet SaeC was critical for localization of major ESX-1 components. Together, these observations suggest that SaeC is both an early recruit and recruiter to the cell pole in ESX-1 assembly. SaeC does not appear to be secreted, as it is not detected in culture filtrates (Fig. S5). Future studies will focus on the role of SaeC (and SaeA,B) in the mechanism and order of ESX-1<sub>ms</sub> assembly, and whether ESX-1<sub>mt</sub> assembly requires a comparable activity. The localization of ESX-1 at the site of active cell-wall synthesis suggests that ESX-1 secretion may function in the generation or modification of the mycobacterial cell wall. Such a relationship might explain the myriad effects attributed to ESX-1 in microbe-environment interactions.



## Experimental procedures

### Bacterial strains, plasmids and media

*E. coli* DH5 $\alpha$  (Invitrogen), *E. coli* XL10Gold (Stratagene), and ER2925 (New England BioLabs) were used for all experiments to propagate plasmid DNA constructs. *E. coli* strains were cultured in Terrific Broth or on Luria-Bertani agar at 37°C, supplemented with antibiotics, as necessary, at the following concentrations: Apramycin 50  $\mu\text{g ml}^{-1}$ , Kanamycin 50  $\mu\text{g ml}^{-1}$ , and Hygromycin 100  $\mu\text{g ml}^{-1}$ . *M. smegmatis* donor strains were derivatives of the laboratory strain, mc<sup>2</sup>155, and have been described previously, as has the recipient strain MKD8 (Table S3; Parsons *et al.*, 1998). *M. smegmatis* strains were cultured at 37°C in Trypticase Soy Broth with, or, without 0.05% Tween80 (TSBT and TSB, respectively), or on Trypticase Soy Agar (TSA) plates, supplemented with antibiotics, as necessary, at the following concentrations: Apramycin 50  $\mu\text{g ml}^{-1}$ , Kanamycin 10  $\mu\text{g ml}^{-1}$ , Hygromycin 100  $\mu\text{g ml}^{-1}$ , and Streptomycin 200  $\mu\text{g ml}^{-1}$ .

### Creation of fluorescent protein fusions

A yellow fluorescent protein gene, *YFPVenus*, was PCR amplified using oligonucleotides TGD1536 and TGD1563 (Table S2). *YFPVenus* was cloned into pMP349 (Consaul and Pavelka, 2004) to create the fluorescent protein expression plasmid, pGD15 (Table S1). Failsafe™ Enzyme Mix (EPICENTRE® Biotechnologies) was used to PCR amplify genes of interest from *M. smegmatis* mc<sup>2</sup>155 genomic DNA, or from cell lysates of heat-killed *M. tuberculosis* H37Rv. PCR products were cloned between the MscI and NheI sites of pGD15 to fuse *YFPVenus*, in frame, to the 3' end of the gene. All fusion constructs were sequenced to verify the fusion was in-frame and rule out PCR-induced mutations.

### Creation of bi-cistronic expression plasmid for co-localization studies

A red fluorescent protein gene, *TdTomato*, (Shaner *et al.*, 2004) was PCR amplified and cloned between the BsrGI and EcoRI sites in pGD15, to create pGD15\_TdTomato (Table S1). pGD15\_TdTomato was then used to co-express TdTomato and YFP fusions.

### Microscopy

Fluorescent-protein fusion plasmids were transformed into *M. smegmatis* and colonies were assessed for fluorescence using a Zeiss Stemi SV6 stereomicroscope with a GFP filter (470nm). Fluorescent colonies were individually inoculated into TSBT and TSB, supplemented with 50  $\mu\text{g ml}^{-1}$  Apramycin. Bacterial cells were examined with either a Nikon TE 2000 microscope with a Roper HQ 2-shot color cooled CCD camera or a Zeiss Axiovert 200M, with a Lambda 10-2 Filterwheel shutter controller, plus a Hamamatsu Camera and a Hamamatsu ORCA-ER camera controller; all hardware was controlled with OpenLab software. Image analysis was performed using ImageJ (NIH®) or AdobePhotoshop. Images were normalized for brightness, contrast, and resolution. Cells were scored as having 1 focus, multiple foci, diffuse fluorescence, or no fluorescence (Fig. S2), with blinded evaluation for quantitation.

### Time lapse microscopy

Cells were imaged in a custom flow-cell microfluidic device made of patterned PDMS fused to cover glass, ensuring that the cells were in the focal plane and received fresh media throughout the experiment (Aldridge, B., Fernandez-Suarez, M., Heller, D., Irimia, D., Toner, M., and Fortune, S., 2012). Standard lithography methods were used to manufacture the device. Fluorescent and bright-field images were acquired every ten minutes using a DeltaVision PersonalDV microscope with a heated chamber and a 100 $\times$  objective (Applied Precision Inc.). Three reviewers independently assessed the cells for the appearance of foci

at an old pole, a new pole (associated with recent septation), or ambiguous (could not be properly assigned due to cell movement or clustering).

### Creation of targeting substrates for recombineering

Plasmid constructs to be used as recombination substrates were based on pYUB854 and were introduced into the recombineering strain expressing Che9c recombination genes as described (van Kessel and Hatfull, 2008). Oligonucleotides and recombination plasmid substrates used for deletion of *saeA-C* and *eccCb-essA* are described in Tables S2 and S1 respectively. The Hyg<sup>R</sup> gene used to replace the target gene was excised by ectopic expression of resolvase. Recombinant strains were verified by PCR and DNA sequence analysis of the resolved *res* site junction.

### Filter mating assays

Quantitative DNA transfer experiments were carried out in triplicate and in parallel with wild-type controls as described previously (Parsons et al., 1998). Two recipient-defective mutant strains were used for matings with a wild-type donor MKD6 (Km<sup>R</sup>). A transposon insertion mutant of gene *eccCb<sub>ms</sub>* was described previously (Coros et al., 2008, van Kessel and Hatfull, 2008). A deletion of *saeC* was also created in this study by a two-step process. First, a hyg<sup>R</sup> allelic replacement of *saeC* was made in the donor strain by recombineering, as described above. The hyg<sup>R</sup> marker was then transferred into the recipient strain MKD8 (Sm<sup>R</sup>). The precise nature of the deletion was confirmed by PCR and DNA sequence analysis (data not shown). MKD8Δ*saeC* was defective for transfer as predicted, and could be complemented *in trans* with the wild-type gene.

### Secretion Assay

Secretion assays were performed as described previously (Coros et al, 2008). Briefly, *M. smegmatis* strains were grown in 10 ml of Sauton's media containing 0.05% Tween-80 and grown with shaking at 37°C to 0.6–0.7 OD<sub>600</sub>. Culture supernatants were concentrated using Amicon Ultra-15 centrifugal filters (3 kDa, MW cut-off). Equivalent cell volumes of supernatant and pellet were heat denatured at 95°C for 15 min in SDS loading buffer. Samples were separated on a 4–12% gradient SDS-PAGE gel, transferred to a PVDF membrane (Amersham Hybond-P), and then probed with appropriate antibodies. Secondary antibodies and detection reagents were from Amersham ECL Plus detection kit (GE Healthcare) and were used according to manufacturer's instructions. Anti-EsxB polyclonal antibodies were generated in this laboratory. Anti-GroEL and anti-rabbit antibodies were obtained from Enzo Life Sciences and Pierce/Thermo Scientific, respectively.

### Supplementary Material

Refer to Web version on PubMed Central for supplementary material.

### Acknowledgments

The authors wish to thank the Wadsworth Center Applied Genomic Technologies Core for DNA sequencing; the Light Microscopy Core for assistance with fluorescent microscopy; and the Wadsworth Center Digital Photography, Illustration and Video Unit for assistance with image analysis. Brian Callahan made the initial observations with the *EccCb<sub>mt</sub>*-YFP expression plasmid. SEW was initially supported by an Emerging Infectious Disease Fellow funded by the CDC, and administered by the Association of Public Health Laboratories. Funding was provided by grants AI042308, R56AI080694 and R21AI088792 to KMD and a New Innovator's Award, DP2 0D001378, to SF.

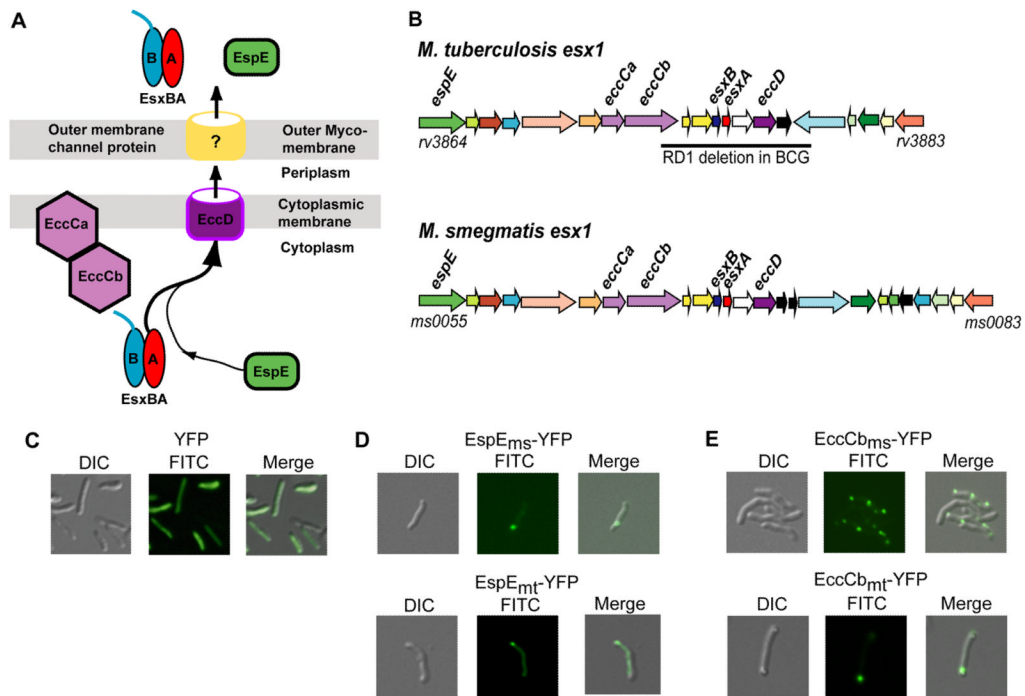
## References

- Abdallah AM, Gey van Pittius NC, Champion PA, Cox J, Luirink J, Vandenbroucke-Grauls CM, Appelmek BJ, Bitter W. Type VII secretion-mycobacteria show the way. *Nat Rev Microbiol*. 2007; 5:883–891. [PubMed: 17922044]
- Aldridge BB, Fernandez-Suarez M, Heller D, Ambravaneswaran V, Irimia D, Toner M, Fortune SM. Asymmetry and aging of mycobacterial cells lead to variable growth and antibiotic susceptibility. *Science*. 2012; 335:100–104. [PubMed: 22174129]
- Behr MA, Wilson MA, Gill WP, Salamon H, Schoolnik GK, Rane S, Small PM. Comparative genomics of BCG vaccines by whole-genome DNA microarray. *Science*. 1999; 284:1520–1523. [PubMed: 10348738]
- Berthet FX, Rauzier J, Lim EM, Philipp W, Gicquel B, Portnoi D. Characterization of the *Mycobacterium tuberculosis* *erp* gene encoding a potential cell surface protein with repetitive structures. *Microbiology*. 1995; 141:2123–2130. [PubMed: 7496523]
- Bitter W, Houben EN, Bottai D, Brodin P, Brown EJ, Cox J, Derbyshire KM, Fortune SM, Gao LY, Liu J, Gey van Pittius NC, Pym AS, Rubin EJ, Sherman DR, Cole ST, Brosch R. Systematic genetic nomenclature for Type VII secretion systems. *PLoS Pathog*. 2009; 5:e1000507. [PubMed: 19876390]
- Burton B, Dubnau D. Membrane-associated DNA transport machines. *Cold Spring Harb Perspect Biol*. 2010; 2:a000406. [PubMed: 20573715]
- Carlsson F, Joshi SA, Rangell L, Brown EJ. Polar localization of virulence-related Esx-1 secretion in mycobacteria. *PLoS Pathog*. 2009; 5:e1000285. [PubMed: 19180234]
- Christie PJ, Atmakuri K, Krishnamoorthy V, Jakubowski S, Cascales E. Biogenesis, architecture and function of bacterial Type IV secretion systems. *Annual Review of Microbiology*. 2005; 59:451–485.
- Consaul SA, Pavelka MS Jr. Use of a novel allele of the *Escherichia coli* *aacC4* aminoglycoside resistance gene as a genetic marker in mycobacteria. *FEMS Microbiol Lett*. 2004; 234:297–301. [PubMed: 15135536]
- Converse SE, Cox JS. A protein secretion pathway critical for *Mycobacterium tuberculosis* virulence is conserved and functional in *Mycobacterium smegmatis*. *J Bacteriol*. 2005; 187:1238–1245. [PubMed: 15687187]
- Coros A, Callahan B, Battaglioli E, Derbyshire KM. The specialized secretory apparatus ESX-1 is essential for DNA transfer in *Mycobacterium smegmatis*. *Mol Microbiol*. 2008; 69:794–808. [PubMed: 18554329]
- DiGiuseppe Champion PA, Cox JS. Protein secretion systems in Mycobacteria. *Cell Microbiol*. 2007; 9:1376–1384. [PubMed: 17466013]
- Edgar R, Rokney A, Feeney M, Semsey S, Kessel M, Goldberg MB, Adhya S, Oppenheim AB. Bacteriophage infection is targeted to cellular poles. *Mol Microbiol*. 2008; 68:1107–1116. [PubMed: 18363799]
- Ehrt S, Guo XV, Hickey CM, Ryou M, Monteleone M, Riley LW, Schnappinger D. Controlling gene expression in mycobacteria with anhydrotetracycline and Tet repressor. *Nucleic Acids Res*. 2005; 33:e21. [PubMed: 15687379]
- Flardh K. Cell polarity and the control of apical growth in *Streptomyces*. *Curr Opin Microbiol*. 2010; 13:758–765. [PubMed: 21036658]
- Flint JL, Kowalski JC, Karnati PK, Derbyshire KM. The RD1 virulence locus of *Mycobacterium tuberculosis* regulates DNA transfer in *Mycobacterium smegmatis*. *Proc Natl Acad Sci U S A*. 2004; 101:12598–12603. [PubMed: 15314236]
- Fortune SM, Jaeger A, Sarracino DA, Chase MR, Sassetti CM, Sherman DR, Bloom BR, Rubin EJ. Mutually dependent secretion of proteins required for mycobacterial virulence. *Proc Natl Acad Sci U S A*. 2005; 102:10676–10681. [PubMed: 16030141]
- Gey Van Pittius NC, Gamielidien J, Hide W, Brown GD, Siezen RJ, Beyers AD. The ESAT-6 gene cluster of *Mycobacterium tuberculosis* and other high G+C Gram-positive bacteria. *Genome Biol*. 2001; 2:1–18.

- Hahn J, Maier B, Haijema BJ, Sheetz M, Dubnau D. Transformation proteins and DNA uptake localize to the cell poles in *Bacillus subtilis*. *Cell*. 2005; 122:59–71. [PubMed: 16009133]
- Hayes CS, Aoki SK, Low DA. Bacterial contact-dependent delivery systems. *Annu Rev Genet*. 2010; 44:71–90. [PubMed: 21047256]
- Hsu T, Hingley-Wilson SM, Chen B, Chen M, Dai AZ, Morin PM, Marks CB, Padiyar J, Goulding C, Gingery M, Eisenberg D, Russell RG, Derrick SC, Collins FM, Morris SL, King CH, Jacobs WR Jr. The primary mechanism of attenuation of bacillus Calmette-Guerin is a loss of secreted lytic function required for invasion of lung interstitial tissue. *Proc Natl Acad Sci U S A*. 2003; 100:12420–12425. [PubMed: 14557547]
- Judd PK, Kumar RB, Das A. Spatial location and requirements for the assembly of the *Agrobacterium tumefaciens* type IV secretion apparatus. *Proc Natl Acad Sci U S A*. 2005; 102:11498–11503. [PubMed: 16076948]
- Kaufenstein M, van der Laan M, Graumann PL. The three-layered DNA uptake machinery at the cell pole in competent *Bacillus subtilis* cells is a stable complex. *J Bacteriol*. 2011; 193:1633–1642. [PubMed: 21278288]
- Kutter S, Buhrdorf R, Haas J, Schneider-Brachert W, Haas R, Fischer W. Protein subassemblies of the *Helicobacter pylori* Cag Type IV secretion system revealed by localization and interaction studies. *J Bacteriol*. 2008; 190:2161–2171. [PubMed: 18178731]
- Lenarcic R, Halbedel S, Visser L, Shaw M, Wu LJ, Errington J, Marenduzzo D, Hamoen LW. Localisation of DivIVA by targeting to negatively curved membranes. *EMBO J*. 2009; 28:2272–2282. [PubMed: 19478798]
- Lewis KN, Liao R, Guinn KM, Hickey MJ, Smith S, Behr MA, Sherman DR. Deletion of RD1 from *Mycobacterium tuberculosis* mimics bacille Calmette-Guerin attenuation. *J Infect Dis*. 2003; 187:117–123. [PubMed: 12508154]
- MacGurn JA, Raghavan S, Stanley SA, Cox JS. A non-RD1 gene cluster is required for Snm secretion in *Mycobacterium tuberculosis*. *Mol Microbiol*. 2005; 57:1653–1663. [PubMed: 16135231]
- Mahairas GG, Sabo PJ, Hickey MJ, Singh DC, Stover CK. Molecular analysis of genetic differences between *Mycobacterium bovis* BCG and virulent *M. bovis*. *J Bacteriol*. 1996; 178:1274–1282. [PubMed: 8631702]
- Nagai T, Ibata K, Park ES, Kubota M, Mikoshiba K, Miyawaki A. A variant of yellow fluorescent protein with fast and efficient maturation for cell-biological applications. *Nat Biotechnol*. 2002; 20:87–90. [PubMed: 11753368]
- Pallen MJ. The ESAT-6/WXG100 superfamily -- and a new Gram-positive secretion system? *Trends Microbiol*. 2002; 10:209–212. [PubMed: 11973144]
- Papanikou E, Karamanou S, Economou A. Bacterial protein secretion through the translocase nanomachine. *Nat Rev Microbiol*. 2007; 5:839–851. [PubMed: 17938627]
- Parsons LM, Jankowski CS, Derbyshire KM. Conjugal transfer of chromosomal DNA in *Mycobacterium smegmatis*. *Mol Micro*. 1998; 28:571–582.
- Pym AS, Brodin P, Brosch R, Huerre M, Cole ST. Loss of RD1 contributed to the attenuation of the live tuberculosis vaccines *Mycobacterium bovis* BCG and *Mycobacterium microti*. *Mol Microbiol*. 2002; 46:709–717. [PubMed: 12410828]
- Ramamurthi KS. Protein localization by recognition of membrane curvature. *Curr Opin Microbiol*. 2010; 13:753–757. [PubMed: 20951078]
- Ramamurthi KS, Lecuyer S, Stone HA, Losick R. Geometric cue for protein localization in a bacterium. *Science*. 2009; 323:1354–1357. [PubMed: 19265022]
- Renshaw PS, Panagiotidou P, Whelan A, Gordon SV, Hewinson RG, Williamson RA, Carr MD. Conclusive evidence that the major T-cell antigens of the *Mycobacterium tuberculosis* complex ESAT-6 and CFP-10 form a tight, 1:1 complex and characterization of the structural properties of ESAT-6, CFP-10, and the ESAT-6-CFP-10 complex. Implications for pathogenesis and virulence. *J Biol Chem*. 2002; 277:21598–21603. [PubMed: 11940590]
- Reuther J, Gekeler C, Tiffert Y, Wohlleben W, Muth G. Unique conjugation mechanism in mycelial streptomycetes: a DNA-binding ATPase translocates unprocessed plasmid DNA at the hyphal tip. *Mol Microbiol*. 2006; 61:436–446. [PubMed: 16776656]

- Rokney A, Shagan M, Kessel M, Smith Y, Rosenshine I, Oppenheim AB. *E. coli* transports aggregated proteins to the poles by a specific and energy-dependent process. *J Mol Biol.* 2009; 392:589–601. [PubMed: 19596340]
- Shaner NC, Campbell RE, Steinbach PA, Giepmans BN, Palmer AE, Tsien RY. Improved monomeric red, orange and yellow fluorescent proteins derived from *Discosoma* sp. red fluorescent protein. *Nat Biotechnol.* 2004; 22:1567–1572. [PubMed: 15558047]
- Simeone R, Bottai D, Brosch R. ESX/Type VII secretion systems and their role in host-pathogen interaction. *Curr Opin Microbiol.* 2009; 12:4–10. [PubMed: 19155186]
- Stover CK, de la Cruz VF, Fuerst TR, Burlein JE, Benson LA, Bennett LT, Bansal GP, Young JF, Lee MH, Hatfull GF, et al. New use of BCG for recombinant vaccines. *Nature.* 1991; 351:456–460. [PubMed: 1904554]
- Tseng TT, Tyler BM, Setubal JC. Protein secretion systems in bacterial-host associations, and their description in the Gene Ontology. *BMC Microbiol.* 2009; 9(Suppl 1):S2. [PubMed: 19278550]
- van Kessel JC, Hatfull GF. Mycobacterial recombineering. *Methods Mol Biol.* 2008; 435:203–215. [PubMed: 18370078]
- Zhu W, Banga S, Tan Y, Zheng C, Stephenson R, Gately J, Luo ZQ. Comprehensive identification of protein substrates of the Dot/Icm Type IV transporter of *Legionella pneumophila*. *PLoS One.* 2011; 6:e17638. [PubMed: 21408005]



**Fig. 1.**

*M. smegmatis* and *M. tuberculosis* Esx-1 proteins localize to a cell pole in *M. smegmatis* cells. (A) Model of the ESX-1 secretion apparatus identifying key proteins discussed in this work. EccCab is an ATPase thought to deliver the EsxA and EsxB heterodimer, and associated proteins, to the pore (EccD). The pore components of the outer membrane are unknown. For simplicity, only one (EspE) of the many proteins co-secreted with EsxAB is shown. (B) Comparative genetic map of the *esx1* operons of *M. smegmatis* and *Mtb*, highlighting key genes. Gene orthologs and paralogs are colour coded. The bar below the *Mtb* map indicates the deletion found in *M. bovis*(BCG) resulting in its attenuation. (C–E) Differential interference contrast (DIC, left panel), FITC (center), and merged (right) images of *M. smegmatis* showing that YFP is distributed throughout the cells (C), while YFP-tagged *EspE<sub>ms</sub>* or *EspE<sub>mt</sub>* (D), and the ESX-1-associated ATPase, *EccCb<sub>ms</sub>*, and its *Mtb* orthologue, *EccCb<sub>mt</sub>* (E), localize to the polar regions of *M. smegmatis* cells. 630X total magnification.

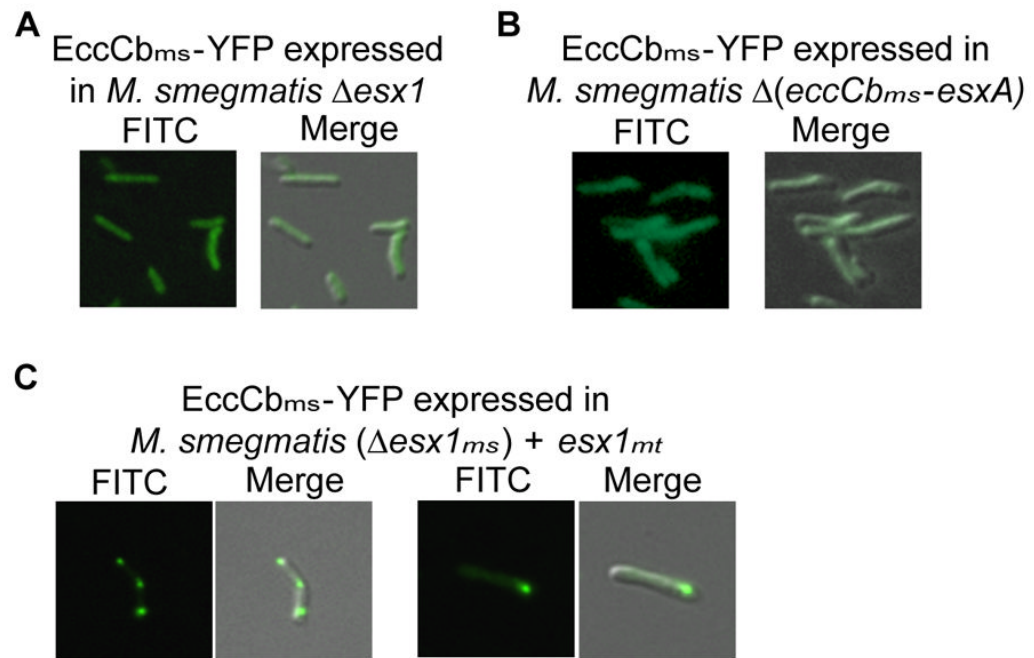


**Fig. 2.** Localization of EccCb<sub>ms</sub> is dependent on other ESX-1-associated proteins. In an *M. smegmatis*  $\Delta$ *esx1* mutant, (**A**), or a  $\Delta$ *eccCb*-*esxA* mutant (**B**), EccCb<sub>ms</sub>-YFP no longer assembled at the cell pole and appeared diffuse throughout the cell. Expression of ESX-1<sub>mt</sub> completely restores polar localization of EccCb<sub>ms</sub>-YFP in the absence of ESX-1<sub>ms</sub> (**C**).

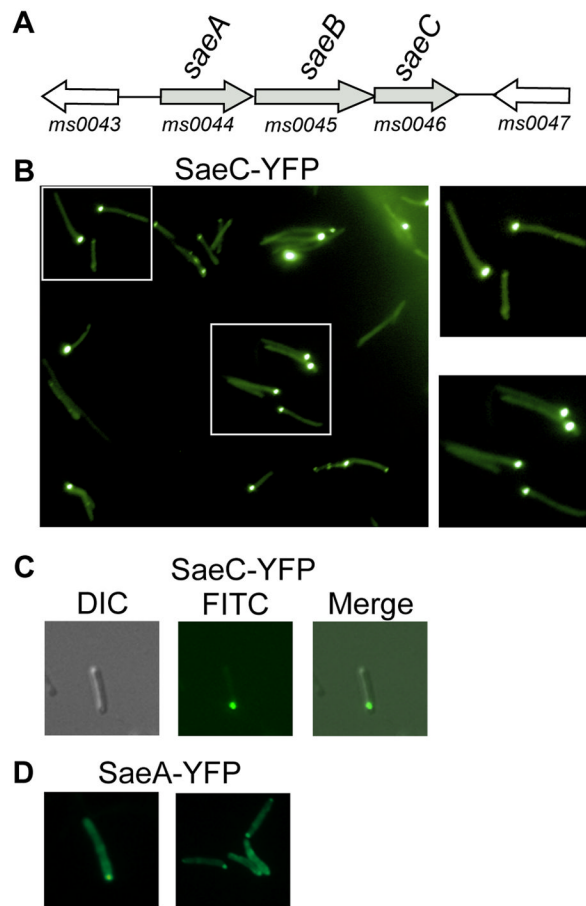


**Fig. 3.** Proteins encoded by the non-*esxI* genes *saeA-C* are essential for ESX-1 function and localize to discrete foci at the cell pole. **(A)** Genetic map of the *sae* operon and flanking genes. **(B)** A wide field FITC image (left panel) showing polar localization of YFP-tagged SaeC, and enlarged images of wild-type bacteria featured in the boxed areas. **(C)** Merged images of a single cell showing YFP-tagged SaeC fluorescing at a cell pole. **(D)** YFP-tagged SaeA is also localized to cell poles. 630× total magnification.

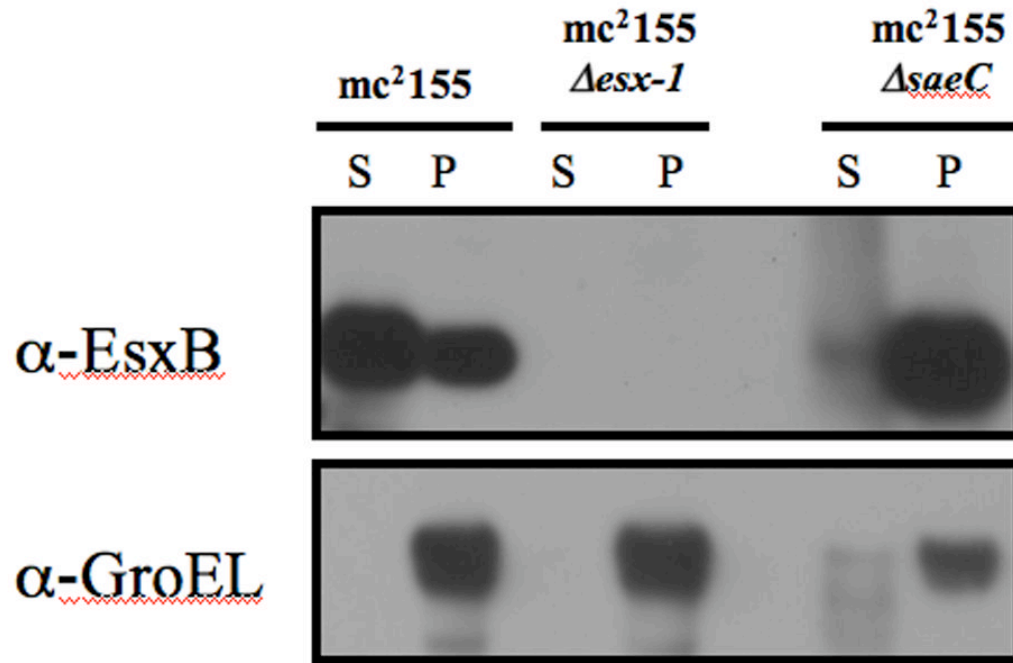


**Fig. 4.** SaeC is required for EsxB secretion. The top panel shows that *mc<sup>2</sup>155* expresses and secretes EsxB into the culture supernatant (S). By contrast, in the *mc<sup>2</sup>155ΔsaeC* deletion strain, EsxB accumulates in the cell pellet (P), indicating SaeC is required for EsxB secretion. The *esx1* deletion strain does not express EsxB. The lower panel demonstrates that GroEL (a marker for cytoplasmic proteins) was detected primarily in the cell pellet, indicating very little cell leakage occurred into the culture filtrate.

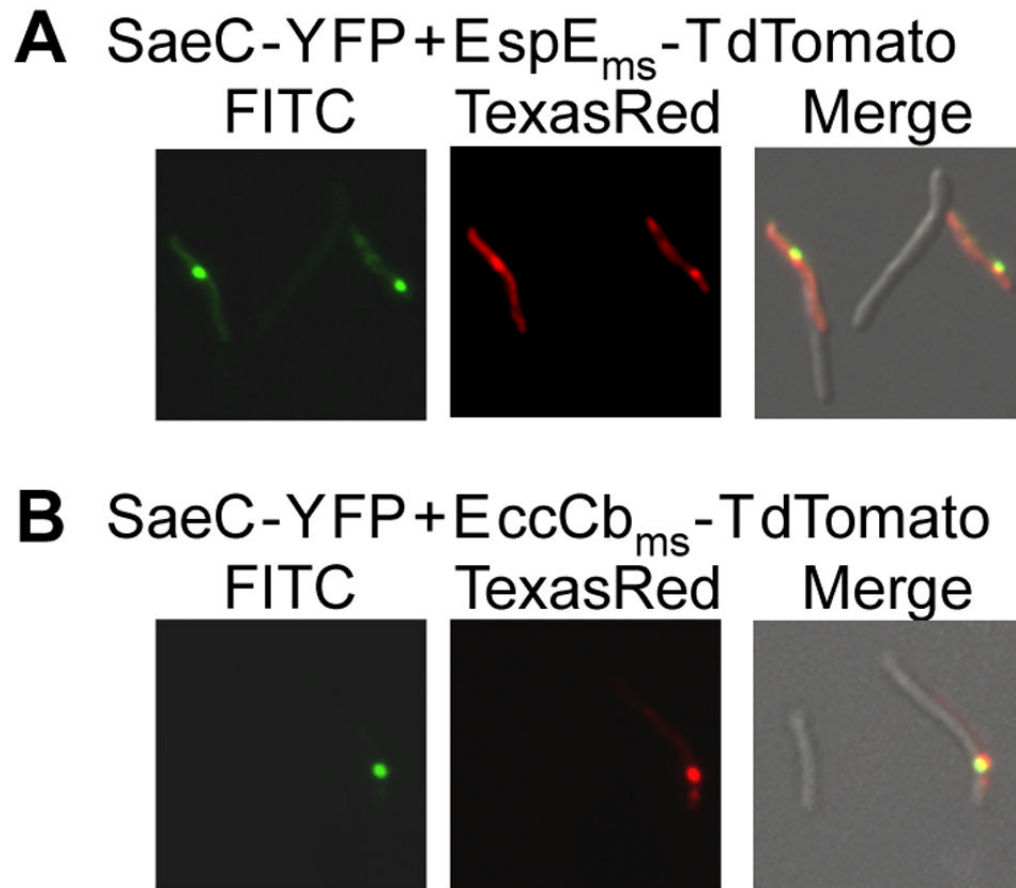


**Fig. 5.** Proteins crucial to ESX-1 function co-localize in the polar region of *M. smegmatis* cells. **(A)** The non-*esx1*-encoded protein, SaeC-YFP, and EspE<sub>ms</sub>-TdTomato co-localize when co-expressed in the same wild-type cell. **(B)** SaeC-YFP also co-localizes with EccCb<sub>ms</sub>-TdTomato in the polar region. 630× total magnification



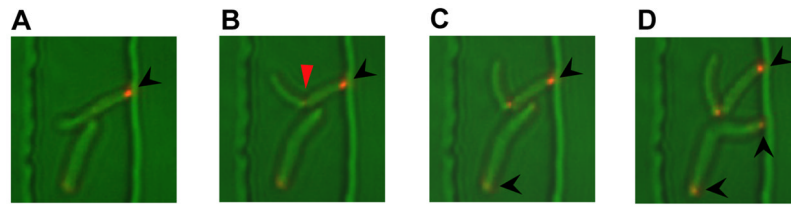


**Fig. 6.** ESX-1 primarily associates with the “old” cell pole. SaeC-YFP localized to the old cell pole of *M. smegmatis* mc<sup>2</sup>155 cells. Bacteria were loaded into a heated flow-cell growth environment and fluorescent images were captured every 10 minutes (**A to D**) with a semi-automated imaging system. Black arrows, old pole. Red arrow, site of new (septal) pole.

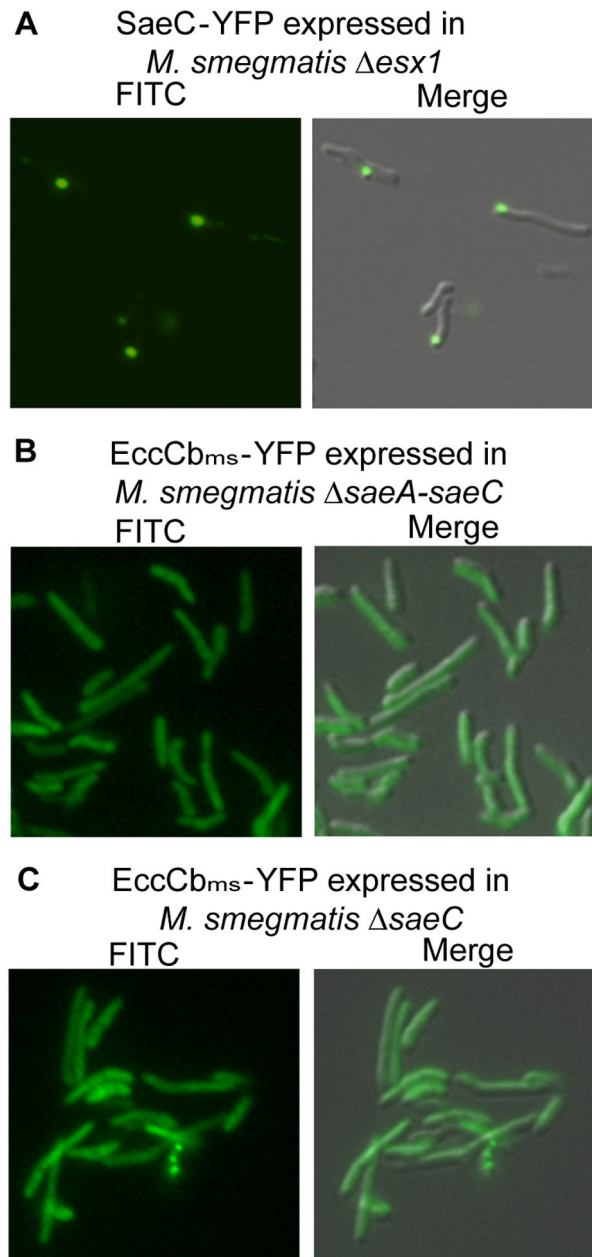


**Fig. 7.** Localization of EccCb<sub>ms</sub> is dependent on SaeC, but localization of SaeC is not dependent on ESX-1. SaeC, localizes to the poles in the absence of ESX-1 core components ( $\Delta esx1$ ) (A). EccCb<sub>ms</sub>-YFP was not localized in either a  $\Delta saeA-saeC$  (B), or a  $\Delta saeC$  mutant background (C), 630 $\times$  total magnification.

**Table 1**

Results of filter mating assays.

Conjugation pair (selectable marker)	Transfer frequency of recipient (transconjugants/recipients) *
MKD6 (Km) × MKD8 (Sm)	$1.02 \times 10^{-4} \pm 0.6$
MKD6 (Km) × MKD8 $\Delta$ <i>saeC</i> (Hyg)	$< 1.00 \times 10^{-9} \pm 0$ **
MKD6 (Km) × MKD8 $\Delta$ <i>saeC</i> + <i>saeC</i> (Apy)	$7.7 \times 10^{-6} \pm 0.6$
MKD6 (Km) × MKD8 $\Delta$ <i>saeC</i> + <i>saeC</i> -YFP (Apy)	$9.0 \times 10^{-6} \pm 0.5$

\* values are the average of at least 3 mating experiments

\*\* no transconjugants were detected after 8 separate mating experiments